

Hepatic Parenchymal Changes following Transcatheter Embolization and Chemoembolization in a Rabbit Tumor Model

Yong Wang[‡], Bin Xiong[‡], Bin Liang, Hui Zhao, Hui Li, Jun Qian, Hui-Min Liang, Gan-Sheng Feng, Chuan-Sheng Zheng*

Department of Radiology, Union Hospital, Tongji Medical College, Huazhong University of Science and Technology, Wuhan, P. R. China

Abstract

Objective: To compare the effects of transcatheter arterial chemoembolization (TACE) with transcatheter arterial embolization (TAE) on liver function, hepatic damage, and hepatic fibrogenesis in a rabbit tumor model.

Materials and Methods: Thirty-nine New Zealand white rabbits implanted with VX2 tumors in the left liver lobes were randomly divided into three groups: TAE, TACE, and control group. In the TAE group (n = 15), polyvinyl alcohol particles (PVAs) were used for left hepatic artery embolization. In the TACE group (n = 15), the tumors were treated with left hepatic arterial infusions of a suspension of 10-hydroxycamptothecin and lipiodol, followed by embolization with PVAs. In the control group (n = 9), the animals received sham treatment with distilled water. Serum and liver samples were collected at 6 hours, 3 days and 7 days after treatment. Liver damage was measured using a liver function test and histological analyses. Liver fibrogenesis and hepatic stellate cell (HSC) activation were evaluated using Sirius Red and anti-alpha-smooth muscle actin (α -SMA) immunohistochemical stains.

Results: TACE caused liver injury with greater increases in serum alanine aminotransferase and aspartate aminotransferase levels on day 3 ($P < 0.05$). Histological analyses revealed increased hepatic necrosis in adjacent non-tumorous liver tissue from day 3 compared to the TAE group (Suzuki score of 2.33 ± 1.29 versus 1.13 ± 1.18 , $P = 0.001$). HSC activation and proliferation were significantly increased in the TACE group compared to the control group at 3 and 7 days after treatment (0.074 ± 0.014 vs. 0.010 ± 0.006 , and 0.088 ± 0.023 vs. 0.017 ± 0.009 , $P < 0.05$). Sirius Red staining demonstrated a statistically significant increase in collagen deposition in the livers in the TACE group 7 days after embolization compared to the control group (0.118 ± 0.012 vs. 0.060 ± 0.017 , $P = 0.05$).

Conclusion: The results of this animal study revealed that TACE induced prominent hepatocellular damage and hepatic fibrogenesis, which compromised liver function and may be responsible for chronic liver decompensation.

Citation: Wang Y, Xiong B, Liang B, Zhao H, Li H, et al. (2013) Hepatic Parenchymal Changes following Transcatheter Embolization and Chemoembolization in a Rabbit Tumor Model. PLoS ONE 8(8): e70757. doi:10.1371/journal.pone.0070757

Editor: Wael El-Rifai, Vanderbilt University Medical Center, United States of America

Received: February 8, 2013; **Accepted:** June 22, 2013; **Published:** August 14, 2013

Copyright: © 2013 Wang et al. This is an open-access article distributed under the terms of the Creative Commons Attribution License, which permits unrestricted use, distribution, and reproduction in any medium, provided the original author and source are credited.

Funding: This study was supported by grants (30970804) from National Natural Sciences Foundation of China and grants from Hubei Provincial Key Laboratory of Molecular Imaging (No. 02.03.2011-78). The funders had no role in study design, data collection and analysis, decision to publish, or preparation of the manuscript.

Competing Interests: The authors have declared that no competing interests exist.

* E-mail: hqzcsxh@sina.com

[‡] These authors contributed equally to this work.

Introduction

Transcatheter arterial embolization (TAE) and chemoembolization (TACE) have been increasingly used as effective palliative treatments for unresectable hepatic tumors [1–3]. TAE and TACE induce ischemic or toxic injury both in the tumors and in the adjacent hepatic tissues, which sometimes results in hepatic failure. Recent studies have suggested that the damage to normal liver parenchyma may impair the therapeutic efficacy of TAE and TACE. Therefore, a thorough understanding of hepatic pathology following transarterial therapy may be helpful for the preservation of liver function.

There has been some speculation regarding the possible causes of TAE- and TACE-induced liver damage. Numerous studies

have concentrated mainly on hepatocyte necrosis [4,5], bile ductal or portal vein endothelial damage [6–8], and inflammatory reactions [9,10]. Liver fibrogenesis, which may be considered to be a wound healing response to liver injury, is characterized by both a quantitative increase and a qualitative change in extracellular matrix (ECM) composition. During this process, hepatic stellate cells (HSCs) are activated and proliferate, contract, induce matrix degradation, and synthesize collagen. HSC activation and liver fibrogenesis play critical roles in the homeostasis of liver repair, regeneration and fibrosis after liver injury [11,12].

Given the fact that ischemia and chemotherapeutic cytotoxicity are potent stimuli for liver repair, we hypothesized that TACE and

TAE may induce hepatocyte necrosis, activate HSCs and initiate fibrogenesis, which are involved in the pathogenesis of hepatic fibrosis and are responsible for chronic liver decompensation. To test this hypothesis, the effects of TACE and TAE on embolized and unembolized liver tissues were examined using morphometric analyses in a rabbit model.

Materials and Methods

Animal Models and Experimental Design

Adult New Zealand white rabbits, weighing 3.0–3.5 kg, were used in this study. Experiments were performed in compliance with the Ethical Guidelines for the Care and Use of Laboratory Animals, as approved by the Animal Care Committee of Hubei Province, China. The animals were anesthetized with an intravenous injection of 30 mg/kg of sodium pentobarbital, and all efforts were made to minimize suffering.

Thirty-nine New Zealand white rabbits with VX2 tumors that had been transplanted into the livers were used in this study. VX2 tumors were implanted by embedding 1 mm tissue cubes below the left lobe capsule for 17–18 days. Each rabbit was then subjected to one of the following three treatment groups: (1) The TAE group ($n = 15$), in which the tumor bearing liver lobe was embolized using polyvinyl alcohol particles (PVA; Cook, Bloomington, Indiana) that were 150–250 μm in diameter; (2) the TACE group ($n = 15$), in which embolization was performed using PVAs after the infusion of a suspension of 10-hydroxycamptothecin (1 mg/kg) and lipiodol (0.4 ml) (Lipiodol Ultra-Fluid; Guerbet, Paris, France) into the left hepatic artery; and (3) the control group ($n = 9$), which was administered a 0.4 ml distilled water infusion into the left hepatic artery. One-third of the animals in each group were euthanized 6 hours, 3 days, and 7 days after treatment. Liver tissues from the embolized and unembolized lobes were surgically removed and fixed in buffered 10% formalin for the immunohistological examinations.

Magnetic Resonance Imaging

Magnetic resonance imaging (MRI) was performed 17–18 days after tumor implantation (and prior to embolization) using a 1.5 T unit (Magnetom Avanto; Siemens Medical Solutions, Erlangen, Germany). All animals underwent a T2-weighted turbo spin-echo (T2W TSE) sequence, with the following imaging parameters: TR/TE = 3700/87 milliseconds, 4 mm slice thickness, 15% intersection gap, 168 Hz/pixel BW, 200*200 mm² field of view, 320*320 matrix, turbo factor = 11, and averages = 2.

Angiographic Procedures

Angiographic procedures were performed using a Siemens C-arm PowerMobile unit (Angiostar Plus, Siemens Medical

Solutions, Munich, Germany) guidance. After surgically cutting the femoral artery, a 4 Fr vascular sheath (Terumo, Tokyo, Japan) was introduced, a 4-Fr Cobra visceral catheter (Terumo) was used to select the celiac axis, and digital subtraction angiography of the celiac axis was then performed. A 2.7 Fr coaxial catheter system (Terumo) was advanced superselectively into the left hepatic artery. Subsequent interventions were carried out after confirmation of vessel insertion and tumor staining using DSA, which was performed using 2 ml manual injections of full strength contrast media (Omnipaque 350; GE Healthcare, Shanghai, China).

For the TAE group, PVAs that had been reconstituted using contrast media were injected carefully into the left hepatic artery. The embolization endpoint was the complete stasis of antegrade blood flow. For the TACE group, embolization was performed using PVAs after the injection of the mixture of 10-hydroxycamptothecin and lipiodol. Treatment was always restricted to the left lobe during each session for both TAE and TACE. For the control animals, 0.4 ml of distilled water was injected instead of the PVAs.

Blood Tests to Assess Liver Function

Blood samples were collected from all of the rabbits 6 hours, 3 days, and 7 days post-procedure. Plasma levels of alanine aminotransferase (ALT), aspartate aminotransferase (AST) and bilirubin were measured using standard enzymatic procedures.

Immunohistochemistry

Liver tissue samples were fixed in 10% neutral buffered formalin and embedded in paraffin. Serial 5 μm thick liver tissue sections were deparaffinized and subjected to hematoxylin-eosin-saffran, Sirius Red and α -SMA immunohistochemical staining.

For Sirius Red staining, the sections were stained with 1% Picro-Sirius Red (Sigma). After 1 hour of staining, the specimens were dehydrated, cleared, sealed and observed under a polarization microscope.

For immunohistochemical staining, alpha-smooth muscle actin (α -SMA) mouse monoclonal antibodies (Sigma, A2547, dilution: 1/100) were used as the primary antibodies. Immunolabeling was achieved using a Super Sensitive Link-Label Immunohistochemical Detection System (Dako, Glostrup, Denmark). First, the paraffin sections were dewaxed and washed with 3% hydrogen peroxide in methanol at room temperature for 10 minutes to block endogenous peroxidase activity. Then, the slides were incubated successively with the primary antibodies, as defined above, and incubated with a secondary anti-mouse immunoglobulin (Dako) for 30 min at room temperature. The binding reactions were visualized using a DAB (3-3-diaminobenzidine tetrahydrochloride) substrate. Finally, the tissue sections were counterstained with hematoxylin.

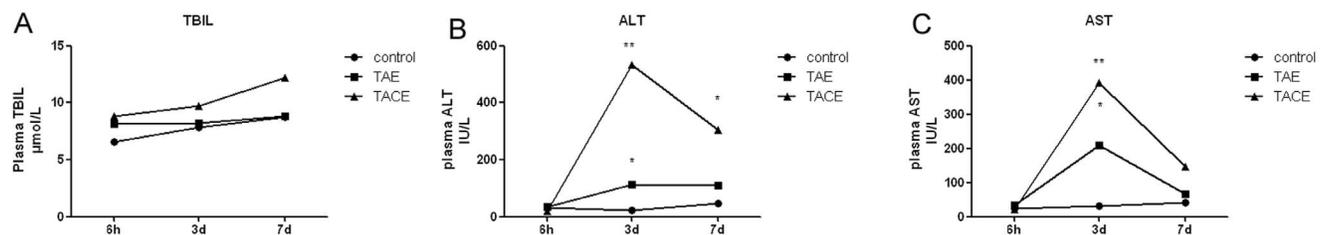


Figure 1. Postoperative changes in serum ALT, AST and bilirubin levels. (A and B) ALT and AST peaked on day 3 in the TAE and TACE groups. (C) Serum bilirubin levels increased slightly after all of the procedures, but these increases were not significant. * $P < 0.05$ compared to the control group; ** $P < 0.05$ compared to the TAE and control groups. doi:10.1371/journal.pone.0070757.g001

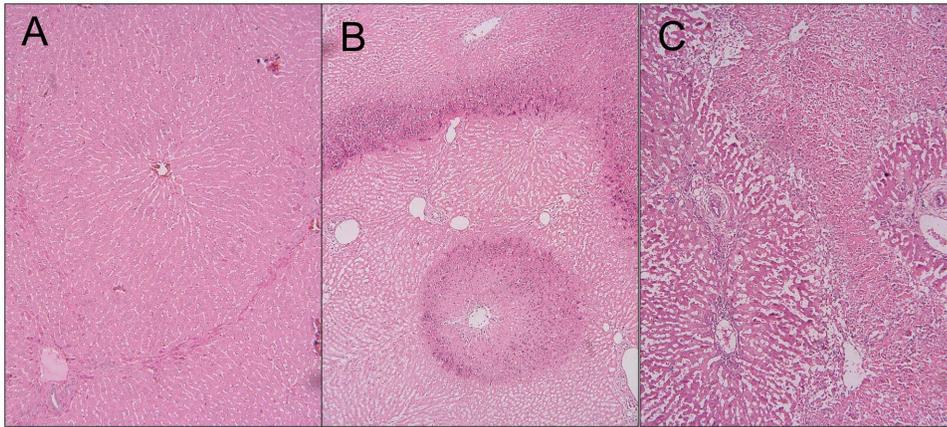


Figure 2. Histologic analyses on postoperative day 7. Hematoxylin and eosin stained livers adjacent to tumors from rabbits (100X). The lobular architecture in the control group was well preserved, and no edema, congestion, or centrilobular necrosis was observed (A). The TAE group displayed focal hepatocyte necrosis and the infiltration of inflammatory cells (B). The TACE group displayed severe sinusoidal congestion and hepatocyte necrosis. Diffuse infiltration of inflammatory cells (lymphocytes and granulocytes) and sinusoidal dilatation/atrophic trabeculae were observed (C). doi:10.1371/journal.pone.0070757.g002

Hepatocellular Necrosis

The severity of liver injury in the left lobes was graded using modified Suzuki's criteria by a researcher who was blinded to the type of procedure that had been performed. In this classification, sinusoidal congestion, hepatocyte necrosis, and ballooning degeneration are graded on a scale from 0 to 4. No necrosis, congestion, or centrilobular ballooning is assigned a score of 0, whereas severe congestion/ballooning and 60% or greater lobular necrosis is assigned a value of 4. Six microscopic fields for each sample were chosen randomly and evaluated at a magnification of 100X.

Liver Fibrogenesis

Sirius Red stains collagen red on a pale yellow background under a bright-field microscope, whereas under a polarization microscope, collagen appears bright yellow-red and/or bright green [1,13]. One section from each specimen, and five fields from each section, were selected randomly. The same measurement procedure was followed for each field, and the mean ratio was then calculated.

α -SMA staining was quantified using morphometric analyses. Labeled areas in the blinded specimens were measured at a video

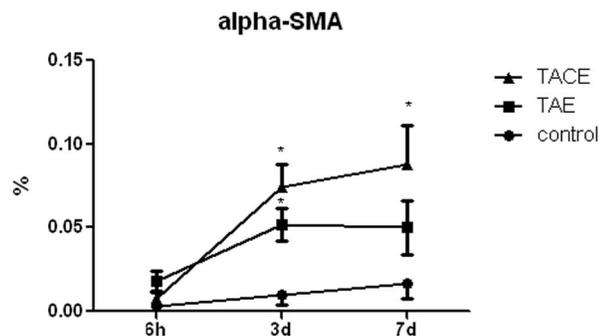


Figure 3. HSC activation following TAE and TACE at different time points after treatment. Areas that stained positive for α -SMA using immunohistochemistry were measured using a computerized image analysis system and expressed as a percentage of the total analyzed area. * $P < 0.05$ vs. control. doi:10.1371/journal.pone.0070757.g003

screen display magnification of 100X and expressed as the ratio of the labeled area per total analyzed field surface. The average of the ratios that were taken from 5 consecutive fields centered on a portal tract was used to generate a single ratio for each specimen.

Statistical Analyses

Quantitative data are presented as the means \pm SD. Significance between groups was established by using the Kruskal-Wallis H and Mann-Whitney U -tests. Differences were considered to be significant if $P < 0.05$. Statistical analyses were carried out using SPSS version 13.0 (SPSS, Chicago, IL).

Results

VX2 Tumor Model

A solitary VX2 tumor was successfully depicted in the left liver lobe of each animal using T2W TSE MRI. The tumor diameter varied from 1.0 to 1.6 cm. TAE and TACE were successfully performed in all animals, and no animals died unexpectedly during the experimental period.

Liver Function

All of the embolized animals showed marked elevations in ALT and AST values on day 3 to levels that were significantly higher than those in the control animals ($P < 0.05$). The ALT and AST values in the animals in the TAE group peaked on day 3 and had decreased by day 7. The rabbits in the TACE group displayed higher levels of ALT and AST than those of the rabbits in the TAE group on day 3 ($P < 0.05$), and higher levels of ALT than the control animals on day 7 ($P = 0.034$). The serum bilirubin values remained similar to control baseline in all of the animals throughout the experimental period [14] (Figures 1A, B, and C).

Hepatic Necrosis

Histopathologic examinations revealed no evidence of apparent hepatic necrosis in the control group. Focal necrosis with sinusoidal congestion and neutrophil accumulation was observed in the midzonal areas in the livers of the animals in the TAE group on days 3 and 7. In contrast, these changes were markedly

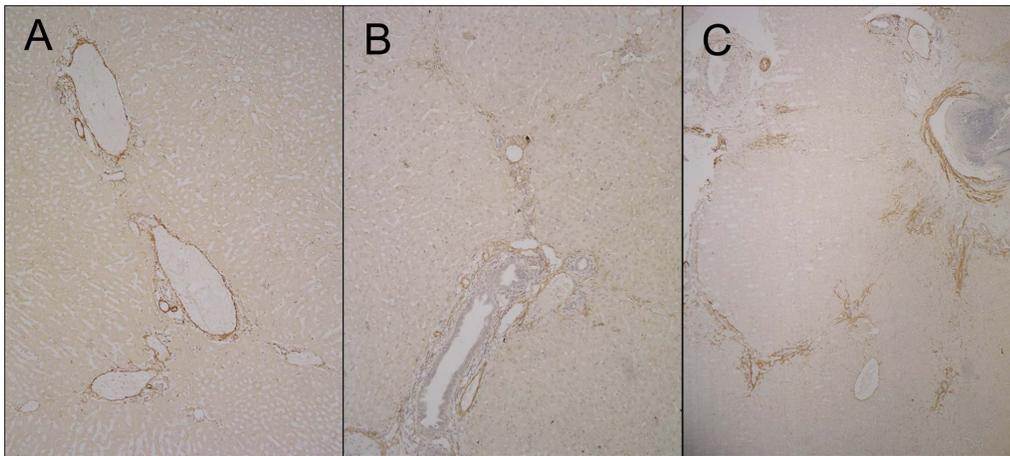


Figure 4. Immunohistochemical staining was used to determine HSC activation using α -SMA. Liver samples (embolized non-tumorous liver tissue) from the control, TAE and TACE groups 3 days after treatment. No positive α -SMA expression was observed in the control group, with the exception of the blood vessels (A). Significant positive α -SMA expression was mainly localized to the hepatic parenchymal cells near the portal tracts in the TAE group (B), and α -SMA expression was higher in the TACE group than in the TAE group (C). doi:10.1371/journal.pone.0070757.g004

increased in the animals in the TACE group at the corresponding times. The extent of hepatic parenchymal necrosis in the animals in the TACE group was significantly higher than that of the animals in the TAE group (Suzuki score of 2.33 ± 1.29 versus 1.13 ± 1.18 , $P = 0.001$). In addition, the extent of hepatic parenchymal necrosis also differed markedly in the animals in the TACE group from the animals in the control group (Suzuki score of 2.33 ± 1.29 versus 0.78 ± 0.67 , $P = 0.006$). The extent of hepatic parenchymal necrosis did not differ between the control and TAE groups [14] (Figures 2A, B, and C).

HSC Activation and Liver Fibrogenesis Following TAE and TACE

Figure 3 shows α -SMA expression after treatment. α -SMA is expressed in activated HSCs and is not expressed in quiescent HSCs [15]. Therefore, we used α -SMA as a reliable marker for HSC activation to determine whether TAE and TACE induced HSC activation. No positive α -SMA expression was detected in the control group, or the unembolized liver tissues in the TAE and TACE groups, with the exception of the blood vessels (Figure 4A).

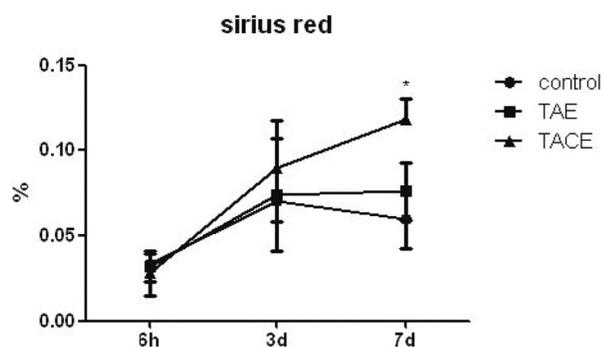


Figure 5. Liver fibrogenesis following TAE and TACE at different time points after treatment. Sirius Red stained areas were measured using a computerized image analysis system and expressed as a percentage of the total analyzed area. * $P < 0.05$ vs. control. doi:10.1371/journal.pone.0070757.g005

No HSC activation was detected in the embolized liver tissues in the TAE and TACE groups 6 hours after treatment. However, on day 3 after TAE or TACE, significant positive α -SMA expression was mainly localized to the hepatic parenchymal cells near the portal tracts (0.052 ± 0.010 and 0.074 ± 0.014 vs. 0.010 ± 0.006 , $P < 0.05$, as compared to the control group), and the expression of α -SMA was even higher in the TACE group than that in the control group by day 7 after treatment (0.088 ± 0.023 vs. 0.017 ± 0.009 , $P = 0.05$) (Figures 4B and C).

Figure 5 shows liver fibrogenesis after treatment. Collagen fibers, as detected using Sirius Red staining, were observed to be concentrated mainly in the connective tissues around the portal tracts in the control group, but not in the hepatic parenchyma (Figure 6A). At hour 6 and day 3 after embolization, the embolized liver tissues did not display discriminatively hepatic parenchymal fibrogenesis. On day 7 after embolization, liver fibrogenesis was detected in the TAE group, but did not differ significantly from that in the control group (Figure 6B). However, collagen fiber staining near the portal tract and central veins was increased in the TACE group (0.118 ± 0.012 vs. 0.060 ± 0.017 , $P = 0.05$) (Figure 6C).

Type III and I collagen fibrils were differentiated based on the different colors of interference and the intensity of collagen birefringence. Against a black background, thick yellow-red fibers were mainly type I collagen, while fine netlike green fibrils were mainly type III collagen. Type II and other tissues were not detected under the polarization microscope. In the control group, type I and III collagen fibrils were confined to the portal area (Figure 6D). In the TAE and TACE groups, alterations in the collagen fibril content, type I in particular, were dramatically observed. The bands of collagen fibrils extended from the portal areas to the hepatic sinuses and dissected liver lobules in these groups (Figures 6E and F).

Discussion

Hepatic stellate cells (HSCs) are a remarkably diverse population of nonparenchymal cells in the liver. After any type of liver injury, HSCs undergo a transformation from cellular quiescence to activation and proliferate at the affected sites, preceding the production of extracellular matrix proteins and hepatic fibrogen-

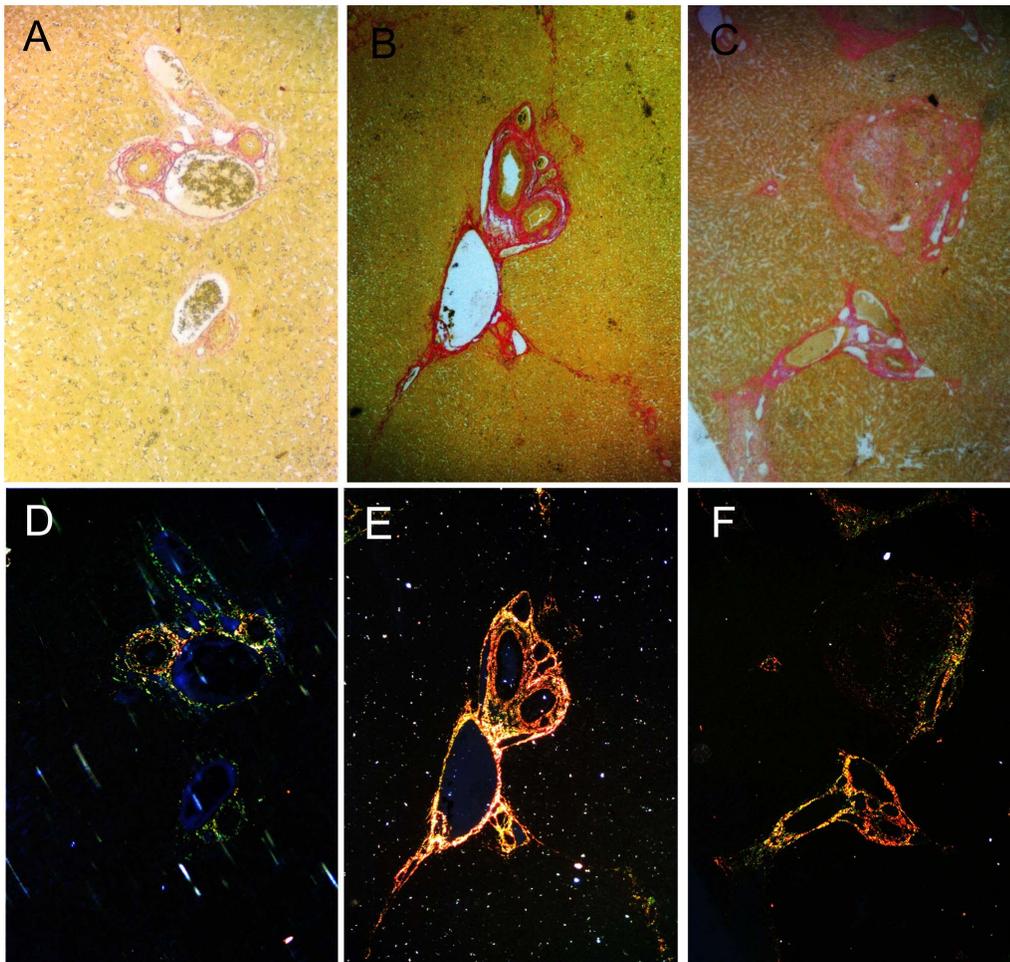


Figure 6. Picro-Sirius Red staining for liver fibrogenesis. Liver samples (embolized non-tumorous liver tissue) from the control, TAE and TACE groups 7 days after treatment. Picro-Sirius Red stains collagen red on a yellow background under a bright-field microscope, whereas under a polarization microscope, collagen appears bright yellow-red (mainly type I collagen), and/or bright green (mainly type III collagen). Seven days after treatment, Picro-Sirius Red staining was observed to be concentrated mainly around the portal tracts in the control group (A), and type I and III collagen fibrils were confined to the portal area (D). Seven days after embolization, liver fibrogenesis was detected in the TAE group (B). However, collagen fiber staining around the portal tracts was increased in the TACE group (C). In the TAE and TACE groups, dramatic increases in the levels of collagen fibrils, type I in particular, were observed (E and F).
doi:10.1371/journal.pone.0070757.g006

esis [16]. Nonsuperselective embolization and chemotherapeutic agent infusion are well known to damage liver tissues (other than neoplastic nodules) and cause hepatocyte necrosis, bile ductal or portal vein endothelial damage, and inflammatory reactions. All of these factors may initiate or accelerate HSC activation and hepatic fibrogenesis.

To our knowledge, very few studies have shown that serum indicators of liver fibrosis, such as procollagen type-III, collagen type-IV, hyaluronate acid and laminin, are elevated after repeated TACE in hepatocellular carcinoma (HCC) patients [17]. Suou et al.[18] demonstrated marked increases in serum levels of the 7S fragment of type IV collagen, and a transient decrease in serum levels of the N-terminal propeptide of type III procollagen, following TAE. These studies reflected the accelerated synthesis and degradation of collagen in the liver that occurs after TAE/TACE. However, no histopathological evidence of liver fibrosis was mentioned. Kobayashi et al.[19] studied the influence of TACE on non-tumorous liver tissue, particularly the portal tract elements, and disclosed that a moderate to marked degree of peribiliary fibrosis frequently occurred in HCC patients who had a

history of TACE compared to controls. However, this study failed to correlate these changes with underlying conditions, including therapies other than TACE, the amounts of embolizing particles, and anticancer drugs. Our study demonstrated that embolization, with or without anticancer drug injection, induced HSC activation and hepatic fibrogenesis in the embolized liver lobes, which participated in the wound healing response to liver damage that was caused by TAE and TACE.

We further investigated the influence of TAE, alone or combined with chemotherapeutic agents, on hepatocyte necrosis, HSC activation and fibrogenesis. In the rabbits in the TAE group, liver function, as assessed by measuring plasma AST, ALT, and bilirubin levels, was not markedly affected. In addition, liver parenchymal necrosis, as observed using histology, was mild, indicating that hepatic arteries that had been embolized with PVAs did not develop prominent hepatocellular damage. Moreover, HSC activation was self-limited and reversible. Hepatic fibrogenesis was not significantly increased during the observation period in the TAE group. In contrast, TACE lead to moderate to severe hepatocellular necrosis in the adjacent

liver tissues, as revealed by significantly increased plasma AST, ALT, and bilirubin levels. Notably, HSC activation increased dramatically between 3 and 7 days in the TACE group as compared to the control group, and collagen levels were increased after 7 days as well. We speculated that the liver damage that was caused by TAE was associated with HSC activation and decreased as injury subsided. When TAE is combined with a mixture of anticancer drugs and ethiodized oil, it not only causes hepatic ischemia, but at the same time also increases the duration of contact between the poison and the non-tumorous liver tissues. Moreover, ethiodized oil may result in the obstruction of the peripheral vascular bed and the portal vein, thereby increasing liver damage [20,21]. Our study provided evidence that the hepatocellular necrosis, HSC activation and fibrogenesis that were induced by TACE were more significant and persistent than those induced by TAE, which may increase the risk of hepatic parenchymal fibrosis.

Two key points that helped us to obtain the results described in this study should be addressed. First, the left hepatic artery was selectively catheterized, and the embolization endpoint chosen in our study was complete stasis of antegrade blood flow, which may have induced hypoxia not only in the tumor, but also in the left lobe. Second, a large quantity of α -SMA expressing cells and collagen fibers were detected in the liver tumors. Therefore, the histological pictures that were used for our analyses were centered on the portal tract area, and the tumor tissues were carefully excluded from the analyzed fields.

Although our experimental model has been generally accepted by many investigators to mimic TAE and TACE [22–24], the majority of cases of liver malignancy in humans, such as hepatocellular carcinoma, develop as a consequence of underlying liver disease (most commonly hepatic cirrhosis). Marked differences in the levels of activated HSCs exist between diseased human livers and normal rabbit livers. Therefore, the influence of TAE and TACE on HSC activation and fibrogenesis in diseased

human livers may not be accurately reflected by our experiments. However, the data that we obtained using our experimental model provided useful information that may be applied to transcatheter treatments that are used for other hepatic tumor types, such as hepatic metastases, in which the background liver tissue is normal. We would also like to mention that the majority of clinical and experimental studies have demonstrated that the liver injury that was caused by TACE was self-limited, that HSC activation decreased over time, and that hepatic fibrogenesis may be reversible, none of which was evaluated in this study.

In summary, the results of the present study provided evidence that HSC activation and hepatic fibrogenesis may contribute to the progression of liver decompensation that is caused by TACE, which suggested that the beneficial effects of TACE in tumor necrosis may be counterbalanced by the deleterious effects of liver fibrosis. These results may shed light on the pathogenesis, treatment and prevention of liver damage that arises from TACE.

Acknowledgments

The authors wish to thank Han-ping Wu in the Department of Radiology, University Hospitals Case Medical Center, Case Western Reserve University, Cleveland, USA, for his valuable revisions and discussion of this manuscript. The authors would also like to thank Yong-hui Yuan in the Department of Pathology, Tongji Medical School, Huazhong University of Science and Technology, Wuhan, China, for his assistance with the immunohistochemical staining, and Dong Chen in the State Key Laboratory Breeding Base of Basic Science of Stomatology, Wuhan, China, for his assistance with the polarization microscopy observations.

Author Contributions

Conceived and designed the experiments: YW BX CZ. Performed the experiments: YW BL HZ. Analyzed the data: YW BX CZ. Contributed reagents/materials/analysis tools: BX H. Li JQ H. Liang GF CZ. Wrote the paper: YW BX CZ.

References

- Chan AO, Yuen MF, Hui CK, Tso WK, Lai CL (2002) A prospective study regarding the complications of transcatheter intraarterial lipiodol chemoembolization in patients with hepatocellular carcinoma. *Cancer* 94: 1747–1752.
- Farinati F, De Maria N, Marafin C, Herszényi L, Del Prato S, et al. (1996) Unresectable hepatocellular carcinoma in cirrhosis: survival, prognostic factors, and unexpected side effects after transcatheter arterial chemoembolization. *Dig Dis Sci* 41: 2332–2339.
- Artinyan A, Nelson R, Soriano P, Chung V, Retseck J, et al. (2008) Treatment response to transcatheter arterial embolization and chemoembolization in primary and metastatic tumors of the liver. *HPB (Oxford)* 10: 396–404.
- Khan KN, Nakata K, Kusumoto Y, Shima M, Ishii N, et al. (1991) Evaluation of nontumorous tissue damage by transcatheter arterial embolization for hepatocellular carcinoma. *Cancer Res* 51: 5667–5671.
- Caturelli E, Siena DA, Fusilli S, Villani MR, Schiavone G, et al. (2000) Transcatheter arterial chemoembolization for hepatocellular carcinoma in patients with cirrhosis: evaluation of damage to nontumorous liver tissue—long-term prospective study. *Radiology* 215: 123–128.
- Chung J, Yu JS, Chung JJ, Kim JH, Kim KW (2010) Haemodynamic events and localised parenchymal changes following transcatheter arterial chemoembolisation for hepatic malignancy: interpretation of imaging findings. *Br J Radiol* 83: 71–81.
- Yu JS, Kim KW, Jeong MG, Lee DH, Park MS, et al. (2002) Predisposing factors of bile duct injury after transcatheter arterial chemoembolization (TACE) for hepatic malignancy. *Cardiovasc Intervent Radiol* 25: 270–274.
- Yu JS, Kim KW, Park MS, Yoon SW (2001) Bile duct injuries leading to portal vein obliteration after transcatheter arterial chemoembolization in the liver: CT findings and initial observations. *Radiology* 221: 429–436.
- Itoh Y, Okanoue T, Ohnishi N, Nishioji K, Sakamoto S, et al. (1999) Hepatic damage induced by transcatheter arterial chemoembolization elevates serum concentrations of macrophage-colony stimulating factor. *Liver* 19: 97–103.
- Kaneko A, Hayashi N, Tanaka Y, Ito T, Kasahara A, et al. (1992) Changes in serum human hepatocyte growth factor levels after transcatheter arterial embolization and partial hepatectomy. *Am J Gastroenterol* 87: 1014–1017.
- Reeves HL, Friedman SL (2002) Activation of hepatic stellate cells—a key issue in liver fibrosis. *Front Biosci* 7: d808–826.
- Li D, Friedman SL (1999) Liver fibrogenesis and the role of hepatic stellate cells: new insights and prospects for therapy. *J Gastroenterol Hepatol* 14: 618–633.
- Zhang H, Sun L, Wang W, Ma X (2006) Quantitative analysis of fibrosis formation on the microcapsule surface with the use of picro-sirius red staining, polarized light microscopy, and digital image analysis. *J Biomed Mater Res A* 76: 120–125.
- Wang Y, Zheng C, Liang B, Zhao H, Qian J, et al. (2011) Hepatocellular necrosis, apoptosis, and proliferation after transcatheter arterial embolization or chemoembolization in a standardized rabbit model. *J Vasc Interv Radiol* 22: 1606–1612.
- Beaussier M, Wendum D, Schiffer E, Dumont S, Rey C, et al. (2007) Prominent contribution of portal mesenchymal cells to liver fibrosis in ischemic and obstructive cholestatic injuries. *Lab Invest* 87: 292–303.
- Geerts A (2001) History, heterogeneity, developmental biology, and functions of quiescent hepatic stellate cells. *Semin Liver Dis* 21: 311–35.
- Kong J, Dou YC, Xu LF, Liang HM, Wu HP, et al. (2002) The New Method in Inspecting Liver Injury After Repeated Transcatheter Arterial Embolization for Treating Hepatocellular Carcinoma: The Liver Fibrotic Indicator Determined. *Shi Yong Fang She Xue Za Zhi* 18: 312–314.
- Suou T, Yamada S, Kobayashi J, Hoshino U, Nishimuki E, et al. (1993) Changes of serum 7S fragment of type IV collagen and N-terminal propeptide of type III procollagen after transcatheter arterial embolization as a model of acute liver injury. *Hepatology* 18: 809–815.
- Kobayashi S, Nakanuma Y, Matsui O (1994) Histopathology of portal tracts in livers after transcatheter arterial chemoembolization therapy for hepatocellular carcinoma. *J Gastroenterol Hepatol* 9: 45–54.
- Yamashita Y, Torashima M, Oguni T, Yamamoto A, Harada M, et al. (1993) Liver parenchymal changes after transcatheter arterial embolization therapy for hepatoma: CT evaluation. *Abdom Imaging* 18: 352–356.
- Wallace S, Kan Z, Li C (2000) Hepatic chemoembolization: clinical and experimental correlation. *Acta Gastroenterol Belg* 63: 169–173.
- Morimoto K, Sakaguchi H, Tanaka T, Yamamoto K, Anai H, et al. (2008) Transarterial chemoembolization using cisplatin powder in a rabbit model of liver cancer. *Cardiovasc Intervent Radiol* 31: 981–985.

23. Virmani S, Rhee TK, Ryu RK, Sato KT, Lewandowski RJ, et al. (2008) Comparison of hypoxia-inducible factor-1alpha expression before and after transcatheter arterial embolization in rabbit VX2 liver tumors. *J Vasc Interv Radiol* 19: 1483–1489.
24. Liang B, Zheng CS, Feng GS, Wu HP, Wang Y, et al. (2010) Correlation of Hypoxia-Inducible Factor 1alpha with Angiogenesis in Liver Tumors After Transcatheter Arterial Embolization in an Animal Model. *Cardiovasc Intervent Radiol* 33: 806–812.